Available online at www.sciencedirect.com
SCIENCE DIRECT®
PERGAMON
International Journal of Heat and Mass Transfer 46 (2003) 1861–1872
International Journal of HEAT and MASS TRANSFER
www.elsevier.com/locate/ijhmt

Evaporative characteristics of R-134a and R-600a in horizontal tubes with perforated strip-type inserts

Shou-Shing Hsieh *, Kuen-Jang Jang, Huang-Hsiu Tsai

Department of Mechanical and Electro-Mechanical Engineering, National Sun Yat-Sen University, Kaohsiung, Taiwan 80424, China

Received 15 September 2002

Abstract

Experimental heat transfer coefficients for R-134a and R-600a in horizontal tubes with vertically positioned perforated strip-type inserts are reported in this paper. Tests were conducted using a single-tube evaporator test facility. The test section used was 2000 mm long, 10.6 mm inside diameter, horizontal, smooth copper tube with perforated strip-type inserts made from the same material (copper). Test parameters were varied as follows: heat flux 9.1–31.2 kW/m^2; mass velocity 82.3–603.3 kg/m^2 s; quality 0–0.85, and a saturation temperature of 6 °C. The flow pattern were identified for different test tubes and flow conditions. The heat transfer coefficients for R-600a were higher than those for R-134a. The heat transfer performance and pressure drop can be improved up to 2.5 and 1.5, respectively for a 96 perforated holes enhanced tube. All comparisons were based on the same nominal mass flow rate. Finally, an empirical correlation was developed.
© 2003 Elsevier Science Ltd. All rights reserved.

1. Introduction

A lot of work has been carried out to obtain an understanding of boiling heat transfer from a smooth surface. These fundamental studies clearly brought out the complexities of the flow boiling mechanisms, as reviewed by Collier and Thome [1]. At present, many aspects of boiling heat transfer on a smooth surface are well explored, and reasonably good correlations have been developed for the design of efficient heat exchange equipment. However, there are many correlations (over 30) for saturated flow boiling in the literature, some of which were summarized by Kattan et al. [2,3]. With enhanced surfaces, flow boiling heat transfer is further complicated, the heat transfer in horizontal tubes with strip-type inserts has received less attention than that in smooth tube annuli. The lack of design data for heat transfer coefficients, is now one of the limitations in the design of efficient evaporators for use in the refrigeration and process industries [4].

Numerous test data for flow boiling of new refrigerants are now becoming available in the literature. Using 10 electrically heated test sections in series, Hambraeus [5] measured local heat transfer coefficients for R-134a with vapor quality range from 0.1 to 1.0 and found a higher heat transfer rate than that of R-22. Wattelet et al. [6] reported that heat transfer coefficients increases noticeably with increasing vapor quality while the stratified-wavy data were flat.

Several comprehensive studies were performed for micro-finned tubes (for example, Ito and Kimura [7]). Schlager et al. [8] examined three 12.7 mm OD micro-fin tubes having different helix angles (15° to 25°), the average heat transfer coefficients in the micro-fin tubes, based on a nominal equivalent smooth tube area, were 1.6–2.2 times higher than those in smooth tubes. Singh et al. [9] conducted flow boiling observation of R-134a in a micro-fin tube, a transition from a stratified to annular flow occurred at the mass velocity of 100 kg/m^2 s. Recently, Liu [10] experimentally measured the evaporation heat transfer coefficients of R-134a in an axially grooved tube and compared with the corresponding

* Corresponding author. Tel.: +886-7-525-2000; fax: +886-7-525-4215.
E-mail address: sshsieh@mail.nsysu.edu.tw (S.-S. Hsieh).

0017-9310/03/$ - see front matter © 2003 Elsevier Science Ltd. All rights reserved.
PII: S0017-9310(02)00471-4

Nomenclature

A_i	tube inside surface area, mm^2
A_s	strip insert surface area with perforated holes, mm^2
A_t	$A_t = A_i + A_s$, mm^2
Bo	boiling number, $q/h_{fg}G$
D_h	hydraulic diameter based on Yang and Webb [22], mm
D_i	tube inner diameter, mm
f	friction factor
G	mass velocity (flux) based on nominal cross sectional area, kg/m^2 s
h	local two-phase heat transfer coefficient unless otherwise stated, W/m^{2}k
h_{fg}	latent heat of evaporation, kJ/kg
k	thermal conductivity, W/mK
Nu	Nusselt number unless otherwise stated, hD_h/k
P	pressure, kPa
P_R	reduced pressure
q	heat flux, W/m^2
Re	Reynolds number unless otherwise stated, $G(1-x)D_i/\mu_\ell$
t	insert thickness, mm
x	vapor quality
x_0	vapor quality at demarcation point
w	insert width, mm
z	downstream distance, mm

Subscripts

a	enhanced tube
l	liquid
z	at location z along channel length
s	smooth tube
v	vapor
-	average

Greek symbols

Δ	differential
η	A_t/A_i
θ	enhancement factor
μ	viscosity, kg/sm
ρ	mass density, kg/m^3
σ	surface tension, N/m

values of R-22. Hsieh et al. [11] studied the evaporative heat transfer and enhancement performance of serpentine tube experimentally with strip-type insert using R-134a, flow nucleate boiling was found to be enhanced and a lower wall superheat needed for incipient boiling.

Many previous studies examined in-tube evaporative heat transfer enhancement and the associated pressure drop with internally finned tubes. However, in-tube evaporation with strip-type inserts using R-600a as refrigerant has not been examined especially using the strips with perforated holes. In addition, most of the work published for theoretical and empirical two-phase flow patterns were performed with adiabatic air–water systems. There is actual need to characterize two-phase flow patterns in air conditioning and refrigeration applications. The present work is a continuation of our study on evaporative heat transfer and enhancement performance in horizontal tubes with strip-type inserts [11]. Special attention was paid to the effect of the number of perforated holes and effect of the placement/orientation of the insert. In this paper, a correlation relating to saturated flow boiling in horizontal tubes with strip-type inserts, with/without perforated holes with R-600a and R-134a was developed. The sketch of the test inserts, shown in Fig. 1, includes definitions of the pertinent geometric parameters of the four perforated-hole-inserts, as well as a smooth tube used for comparison. The insert surface was coated with very thin silica insulation paint (about 0.05 mm thick) to suppress the fin effect.

2. Experimental setup and procedure

2.1. Test facility

The experimental rig, shown schematically in Fig. 2, was used for heat transfer and pressure drop measurements consisted of the integration of two separate flow loops: (1) a refrigerant loop and (2) a R-22 loop (not shown) which served as a heat sink for the entire rig.

2.1.1. Refrigerant loop

A variable-speed gear pump was used to circulate the refrigerant around the loop, eliminating the need for a compressor and an expansion device used in commercial vapor-compression refrigeration systems. Besides, the R-600a/R-134a loop consisted of a filter, a turbine meter, two heaters (including the preheater), receiver, water bath, and the test section. The locations of thermocouples, pressure taps, and control valves are indicated on the schematic. The refrigerant was completely isolated from the pump lubricant. Therefore, it remained oil-free for all tests. The liquid receiver allowed for stable control of system pressure. The pre-evaporator (not shown) preheated R-600a (R-134a) to saturation

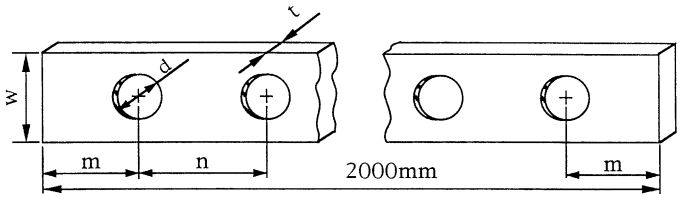

Designated No.	Tube type	D_h (mm)	d (mm)	w (mm)	t (mm)	m (mm)	n (mm)
I	perforated strip 23hole	5.51	6	10	1	65	85
II	perforated strip 54hole	5.64	6	10	1	19.5	37
III	perforated strip 73hole	5.72	6	10	1	14	27
IV	perforated strip 96hole	5.81	6	10	1	12	20.8
	smooth tube	10.6	—	—	—	—	—

(a)

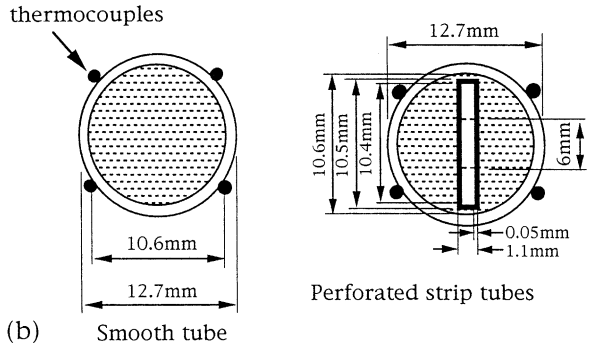

Fig. 1. (a) The geometry of the inserts in the present study and (b) cross-section of test tubes.

(within ±0.1 °C). As R-600a (R-134a) flowed through the test section, it was uniformly heated by DC power, provided by a 200 V, 2 A capacity DC rectifier. Electric resistance was also measured in several stations to ensure uniform heat flux. Autotransformers were used to regulate the heat flux. After exiting the test section, R-600a (R-134a) passed to the R-22 cooled condenser, where it was condensed and subcooled prior to being return to the pump to complete the circuit. The inlet and exit end of the test section has a sight glass, respectively, of almost the same inside diameter as the test section in order to observe the flow conditions and patterns. An enthalpy balance across the flashing valve was used to determine the test section inlet quality. Test section quality at any location was obtained from an energy balance between the enthalpy gain of the fluid and the electrical power dissipation in the test section.

2.1.2. Test section

The test section was a straight, horizontal section having a heated length 2 m with perforated strip-type inserts. All five tubes (including a smooth tube) were made of copper, with an outside diameter of 12.7 mm and an inside diameter 10.6 mm. In addition to the inlet and exit of the test section, instrumentation to measure temperature and pressure was located at intervals of 250 mm. The flow was metered using a turbine flow meter which was chosen for a certain range, from 82.3 to 603.3 $kg/m^2 s$ and calibrated by a stopwatch and bucket method. The pressure and pressure drop were measured with pressure gauges (P) and differential pressure transducers (DP). Bulk fluid temperatures were measured at the inlet and outlet of the test section. The tube wall temperatures were obtained by measuring wall temperature at a certain distance (250 mm each) along downstream locations (see Fig. 2 for details) with 40 gage Cu–Cn thermocouple and with a correction (explained later in the forthcoming section). The wall temperature was measured by four thermocouples circumferentially spaced (90° apart) at these axial downstream locations and an average value was used to calculate the local heat transfer coefficient. The soldering point of the thermocouples to the tube wall was less than 1 mm in diameter. Teflon space dividers were positioned

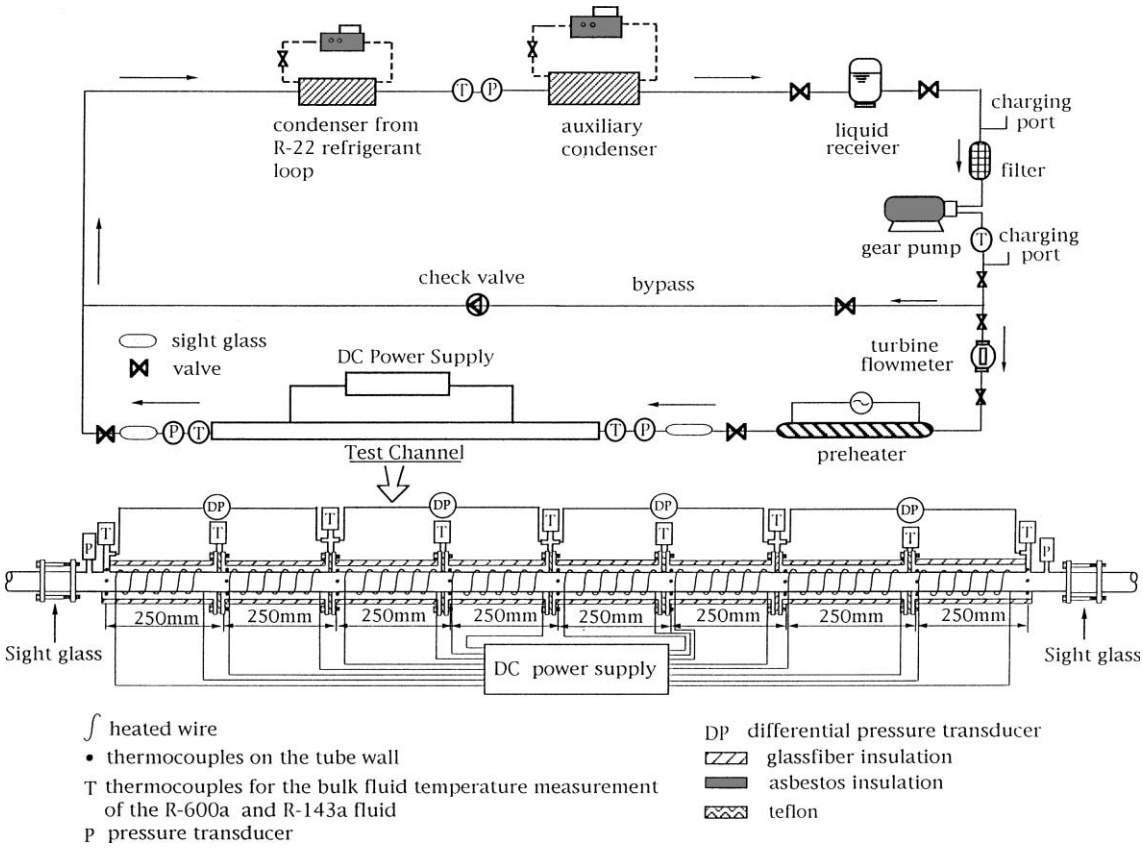

Fig. 2. Schematic of test apparatus and experimental setup.

at intervals of 250 mm along the test section to minimize axial conduction heat losses (<1%).

In each experiment, a 0.5 mm diameter nichrome wire with a pitch of 0.5 mm was circumferentially wound around the tube segmently. The nichrome wire having 5 Ω/m resistance is electrically insulated from the copper tube with 0.4 mm-electrical insulation paper. The heaters are thermally insulated with 35 mm-thick asbestos and 40.0 mm-thick fiberglass insulated to minimize the radial heat gains. The thermocouples have been attached to the back side of the nichrome wire using high thermal conductivity epoxy. In order to avoid biased temperature reading caused by a "fin effect", the thermocouples were also attached to the back of the heating wire over a length of at least 150 mm before being exposed to ambient air. In addition, the thermocouple was aligned with the flow direction to prevent thermal conduction along the tube which could affect the temperature readings. In fact, such conduction heat losses (gains) were found less than 1%.

2.2. Data collection and reduction

The system loop was first evacuated and then charged with refrigerant. The experiments started with a full vacuum in the refrigerant loop and used a careful filling procedure in order to prevent air from entering to the loop. No venting to degas the refrigerant was required under normal conditions. Testing showed that the saturation pressure based on thermocouple readings matched the measured pressure within ±2 kPa, while different pressure drop measurements were accurate to ±0.5 kPa. Thermocouples were calibrated in a thermostatic bath over the testing temperature range, and pressure transducers were calibrated against a known method (e.g. using a U-tube manometer with 25 mm dia. mercury column). The system was tested with single-phase flows and these results were compared with established correlations, see Fig. 3, which is discussed later. The overall heat balance between the electrical heat input (corrected for gains from the surroundings) for single phase flows in the complete test section was found to be within ±2% in the cases under study. Watt transducers were factory calibrated within ±10 W. Refrigerant transport and thermodynamic properties can be obtained from the supplier (ICI Chemicals) and ASHRAE.

The local heat transfer coefficient, at each downstream location z, is defined as $h = q/(T_{wz} - T_{bz})$ where

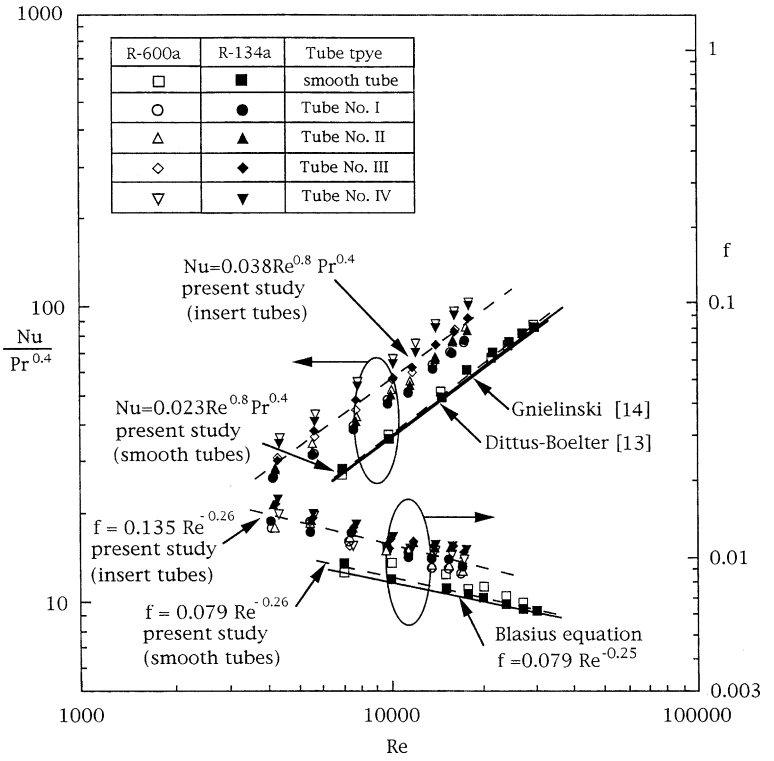

Fig. 3. Single-phase heat transfer characteristics and friction factor in different tubes for R-600a and R-134a.

T_{wz} is the local wall temperature which is taken as the arithmetic mean of four thermocouples installed on the tube wall, T_{bz} is the local measured bulk fluid temperature along the length of the tube for single phase test and is the bulk saturation temperature of the refrigerants corresponding the test section pressure for the flow boiling. q is the inner wall heat flux calculated based on the inside surface area of the tube with/or without insert for performance analysis and easy comparison. The tube wall temperature drop was calculated by considering the steady state, one-dimensional radial heat conduction equation.

For the present study, the circumferential temperature variations were measured to be very small at aforementioned each measured location along the test section. Average heat transfer coefficient and pressure drop data were obtained, respectively, from the average values of the integral of the local heat transfer coefficient and pressure drop along the length of the tube, which were fitted over the vapor quality ranges of 0.002–0.85.

Data collection was performed using an IBM PC and a data acquisition system with data acquisition software. Testing was conducted at steady-state conditions, which were monitored and controlled by the previously mentioned system. Parameters controlled during tests were heat flux, mass velocity (flux), saturation temperature, and insert geometry. It usually takes 1 h to reach a steady state for most cases.

2.3. Uncertainty estimated

The typical uncertainty of the heat transfer coefficients is ±9% using a propagation-of-error analysis [12], while the typical uncertainty of enhancement factors is ±15%. Pressure drop uncertainties were found to be within ±2%. Mass flux has an uncertainty of approximately ±3%, while the typical uncertainty of heat flux is ±0.5%. Uncertainties of the friction factor ranged within ±6%. The uncertainty on the position of the onset of nucleation position was found to be within ±1.5%.

3. Results and discussion

The flow boiling tests were performed at selected values of mass velocity of 83, 166, 239, 356, 475, and 602 kg/m^2 s. The fluid entered the test section as saturated liquid in all tests. The experimental heat flux ranged from 9.1 to 31.2 kW/m^2. Local flow boiling heat transfer coefficients and friction factors for R-134a and R-600a in horizontal tubes with perforated strip-type inserts

(23, 54, 73, and 96 holes) have been examined experimentally.

3.1. Single phase test

Heat gains to the test section were determined through single phase energy balance tests. The results were also checked by comparing forced convection constant heat flux examination with correlations such as that of Dittus–Boelter [13] and Gnielinski [14]. For consistency, Nu and f were calculated based on hydraulic diameter (D_h). Values of single-phase heat transfer coefficients fall within $\pm 6\%$ of these correlations for Reynolds numbers above 10,000 for smooth tubes with R-134a and R-600a, which can be seen in Fig. 3. Also included in Fig. 3 are results for tubes with perforated inserts. The enhancement was clearly observed. The average enhancement factor is 1.65. Similarly, the single phase friction factor was also measured for conditions similar to the test above but without heating. The results indicated in Fig. 3 show that the agreement seems well with the well-known Blasius equation within $\pm 15\%$ for $3000 \leqslant Re \leqslant 30,000$. The factor for pressure drop increase due to inserts is about 1.71.

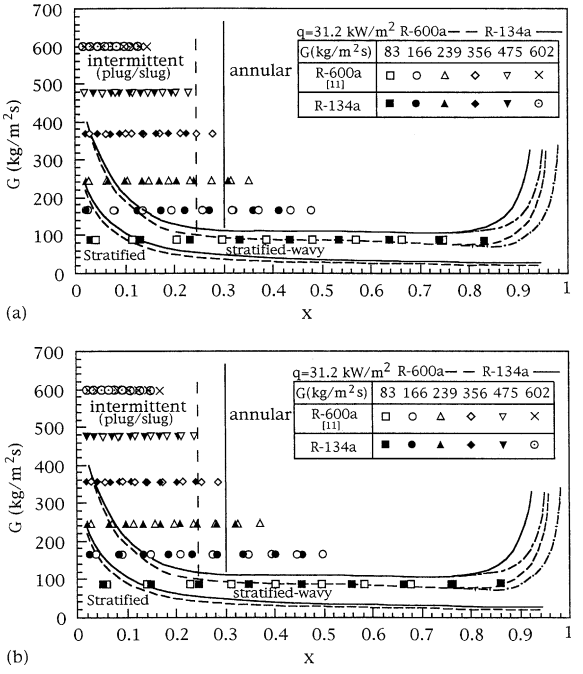

Fig. 4. The flow pattern map for R-600a and R-134a in (a) smooth tubes and (b) perforated strip 96 holes tube.

3.2. Flow map developed

The mechanisms that cause the transition between successive flow patterns need to be identified in order to construct a theoretical map. The transition mechanisms proposed between the three basic flow patterns (intermittent (plug/slug), stratified-wavy, and annular) are discussed and presented here. Application of the flow pattern maps to predict quality at the transition to annular flow indicated that annular flow generally did not start until qualities of 0.3–0.85. Fig. 4(a) shows the flow pattern map following Kattan et al. [15] for the present flow boiling in smooth tubes. It clearly shows that all the present tests seem to be in the annular, intermittent (plug/slug), and stratified-wavy flow regime except at a location upstream 300 mm where bubbly flow regime dominate for $G \leqslant 166$ kg/m^2 s (not shown). Fig. 4(b) presents results for the present tubes with 96 perforated hole inserts for parameters corresponding to that of Fig. 4(a). The R-600a data were obtained from Hsieh et al. [11]. The same behavior as those of the tubes without perforated hole inserts was also observed.

Since the method reported in Kattan et al. [15] does not include the bubble flow regime, the bubble flow regime could not be found in the map. Based on Fig. 4, it seems that almost three-fifths length of the test section is in annular flow regime for all the cases studied. The 166 kg/m^2 s mass velocity with $x \geqslant 0.3$ from Fig. 4 represents the transition value from stratified-wavy flow to annular for the tube with/without insert studied herein. Basically, the present flow pattern shows the same behavior for tubes with/without insert. For instance, all are in stratified, stratified-wang and annular flow regime and have the same threshold transition for intermittent and annular flow. Only the data for tube with insert fall a little bit ahead of those without inserts due to a higher liquid/vapor velocity in tubes with inserts.

The corresponding plot of Fig. 4(a) for $G = 166$ kg/m^2 s and four different heat fluxes, as shown in Fig. 5(a) indicates that the local heat transfer coefficient plotted versus vapor quality raises rapidly as its evaporating liquid film thins at $x \geqslant 0.4$. Under this condition, the demarcation quality x_0 was found to be about 0.4. However, the value is subject to change as the mass velocity is changed. In the stratified-wavy flow regime ($x < 0.4$), the trend in heat transfer coefficient versus vapor quality is an extension to that for annular flow, where it is termed "partial nucleate boiling", and both forced convection and nucleate boiling are significant. The gradual suppression of the latter leads to either a slow increase at low heat flux ($q \leqslant 17.8$ kW/m^2) or temporary reduction at high heat flux ($q \geqslant 26.7$ kW/m^2) of the local heat transfer coefficient. Later, they will increase until finally merging into a single line with increasing vapor quality, in annular flow regime where is also termed forced convection vaporization region. As a result, nucleate boiling at these lower qualities augments the heat transfer coefficient. On the contrary, at higher

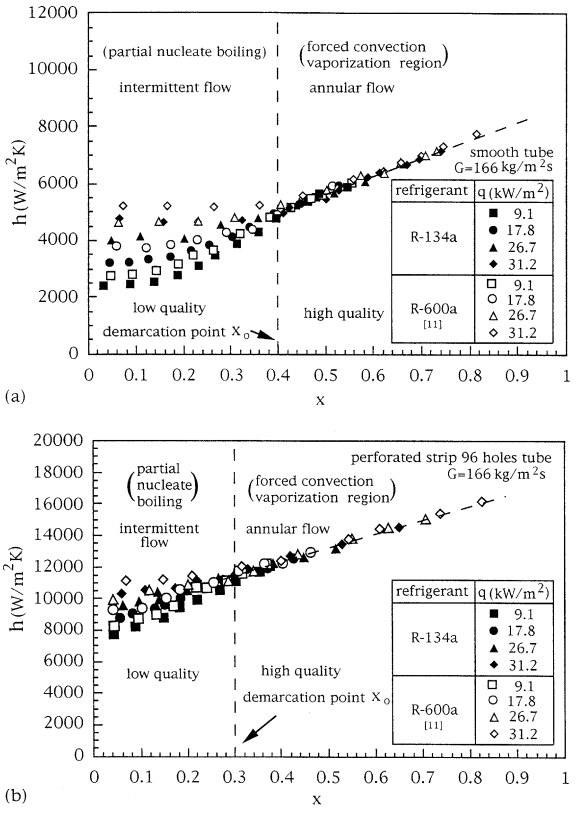

Fig. 5. Local heat transfer coefficient vs. quality at constant mass velocity and different heat flux in (a) smooth tube and (b) perforated strip 96 holes tube.

qualities, nucleate boiling is again largely suppressed due to an annular liquid film thinning. The map shown in Fig. 4 indicates, also the influence of stratification at low flow rates (i.e., $G \leqslant 166$ kg/m^2 s) in the present tubes with/without inserts. In fact, the visual observation (not shown) of the flow indicated that for mass velocities less than 166 kg/m^2 s, the flow was predominantly stratified.

Furthermore, as stated earlier, the demarcation point quality x_0 would be different with different tubes, this time $x_0 = 0.3$ as depicted in Fig. 5(b). Namely, the strip-insert with perforated holes would result in an earlier transition, comparing Fig. 5(a) and (b). In summary, four flow regimes were found based on flow map identification; namely, bubbly, plug/slug, stratified-wavy flow, and annular flow (high mass velocities $G > 166$ kg/m^2 s with $x > 0.3$). That is, the predominant flow pattern was annular flow for higher mass velocity and vapor quality, while stratified-wavy flow predominates for lower mass flux and vapor quality. This finding applies to the two refrigerants tested for both smooth tube and tube with inserts, and is similar to the results of Wattelet [6].

3.3. Heat transfer results

Evaporation tests were carried out at nominal conditions of 190 (R-600a) and 360 (R-134a) kPa (≅6 °C), with mass velocity variations of 83–602 kg/m^2 s. Nominal vapor qualities at the inlet and outlet were about 0–0.85.

3.3.1. Effect of mass flux

Fig. 6 shows evaporation heat transfer results for the four tubes with inserts of differing number of perforated holes at $q = 31.2$ kW/m^2 and also includes the results of the smooth tube for comparison. The heat transfer coefficients for the tubes with inserts were calculated based on the area of a smooth tube. As expected, the heat transfer coefficient increases with increasing mass velocity. Compared with the smooth tube, all four inserted-tubes show a significant increase in heat transfer over the range of mass velocity tested. The effect of inserts on the heat transfer coefficient can be clearly seen in Fig. 6 for five different mass velocities at a given heat flux. In general, an increase in mass velocity increases the heat transfer coefficients for all the qualities plotted. For smooth tubes at $G \leqslant 356$ kg/m^2 s, the heat transfer coefficients were observed to be nearly independent of the quality. In fact, the data of Figs. 5(a) and 6(a) show dominance of the nucleation mechanisms by virtue of the heat flux dependence and nearly mass velocity independence of the data. In contrast, for tubes with inserts and perforated holes, an increase in the quality increases the heat transfer coefficients for all the mass velocities considered herein. This is because the flow in the tubes with inserts was in forced convective boiling in which the heat transfer coefficients would increase as the mass velocity increases.

Taking a closeup examination of Fig. 6, it is also found that the heat transfer coefficient did increase with increasing mass flux at a fixed local mass quality but to a lesser degree than was observed for the smooth tube as evidenced from Fig. 6(a). On the other hand, in spite of the independence of heat flux on h in forced convection vaporization region, the local h depends strongly on the mass flux and the quality as shown in Fig. 6(b)–(e). It is long recognized that heat transfer coefficients are more dependent on heat flux in regions of lower quality ($x < 0.4$), which represents a nucleate boiling region, as compared to a higher quality, which represents a forced convection vaporization region. However, this situation becomes less pronounced for the tubes with inserts. This indicated that an earlier onset of forced convection vaporization can occur with the inserts as mentioned earlier. At $q = 31.2$ kW/m^2, the heat transfer coefficients obtained with the smooth tube drop with quality for $x < 0.1$. This was not observed with the tubes with inserts. At higher qualities the heat transfer coefficient

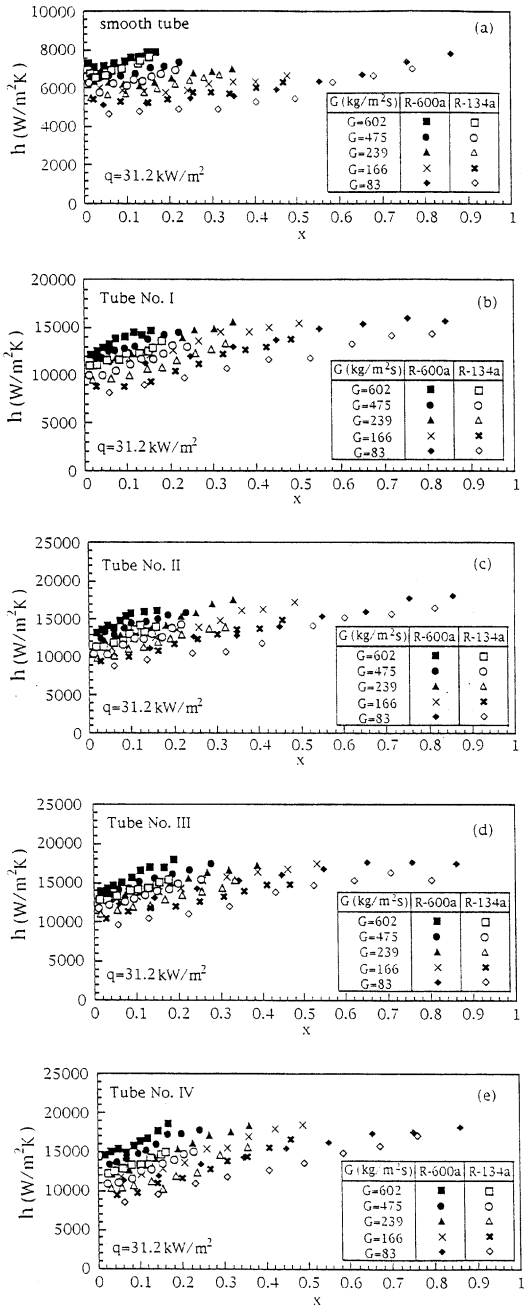

Fig. 6. Local heat transfer coefficient versus quality for different mass flux at $q = 31.2$ kW/m^2.

increases approximately linearly with quality with a slow increase rate especially for the smooth tubes. At this stage, no more bubbles are formed at the wall and heat is conducted by the liquid film with the thickness of liquid film decreasing downstream gradually. Consequently, the heat transfer coefficient increases with the quality. This finding is similar to that of Hsieh et al. [16]. Among four tubes with inserts, tube with 96 perforated holes insert has the highest heat transfer coefficients at $0 \leqslant x \leqslant 0.85$ for all the mass velocities considered under study.

3.3.2. Effect of heat flux

Fig. 7 shows the effect of heat flux on the average heat transfer coefficient. As seen in the figure, the dependence of the coefficient on heat flux is much higher than its dependence on the mass velocity depicted in Fig. 6. The data suggest that the heat transfer coefficients increase gradually with the heat flux. The data obtained in this study were correlated in the form of $\bar{h} = cq^n$. The value of n was found to be about 0.704 which agrees quite well with the value of 0.712 for R-123 reported from Bao et al. [17]. In addition, examination of all the data shows that the slope of the $\bar{h}$ versus q curve is approximately equal for both R-134a and R-600a in the tubes with/without inserts. The heat transfer enhancement for the perforated-hole-inserts was significantly observed for all the cases studied. The rate of increase seems the same at lower and higher heat flux. For instance, at $q = 10$ kW/m^2, $\bar{h}_a/\bar{h}_s \cong 2$ is almost the same as that at $q = 30$ kW/m^2 for the 96-hole-insert when comparing Fig. 7(a) with Fig. 7(d).

3.3.3. Effect of perforated hole and insert placement or orientation

Owing to the heating surface is the tube wall and the fin effect of the insert was suppressed and found to be small, the insert surface effect can be neglected. In addition to the onset of nucleate boiling (discussed earlier), the effect of perforated hole on heat transfer performance was noted at two different heat flux levels ($q = 9.1$ and 31.2 kW/m^2) for both refrigerants. Again, under different G, the performance superiority of R-600a is still obvious and the heat transfer coefficient increases steadily with increases in the number of perforated holes and the mass velocity. This is perhaps due to a change in the contributions between nucleate boiling and convective boiling components. The effect of perforated holes on heat transfer enhancement were also found, $1.6 \leqslant \bar{h}_a/\bar{h}_s \leqslant 3.2$ for $0.04 \leqslant x \leqslant 0.38$ at a lower heat flux, 9.1 kW/m^2 as compared to that ($1.58 \leqslant \bar{h}_a/\bar{h}_s \leqslant 7.5$ for $0.35 \leqslant x \leqslant 0.85$) of higher heat flux, 31.2 kW/m^2. Moreover, the rate of increase for R-600a seems continuously higher than that of R-134a. However, the mass flow effect shows a different trend. Fig. 8(a) and (b) show the plots of $\bar{h}_a/\bar{h}_s$ versus number of holes per unit length at two different heat fluxes. As can be seen, the heat transfer enhancement increases with the number of holes per unit length increase. The curve starts at zero in which there is no hole ($\bar{h}_a/\bar{h}_s = 1$; actually, it is a smooth tube) and gradually increases as the number of

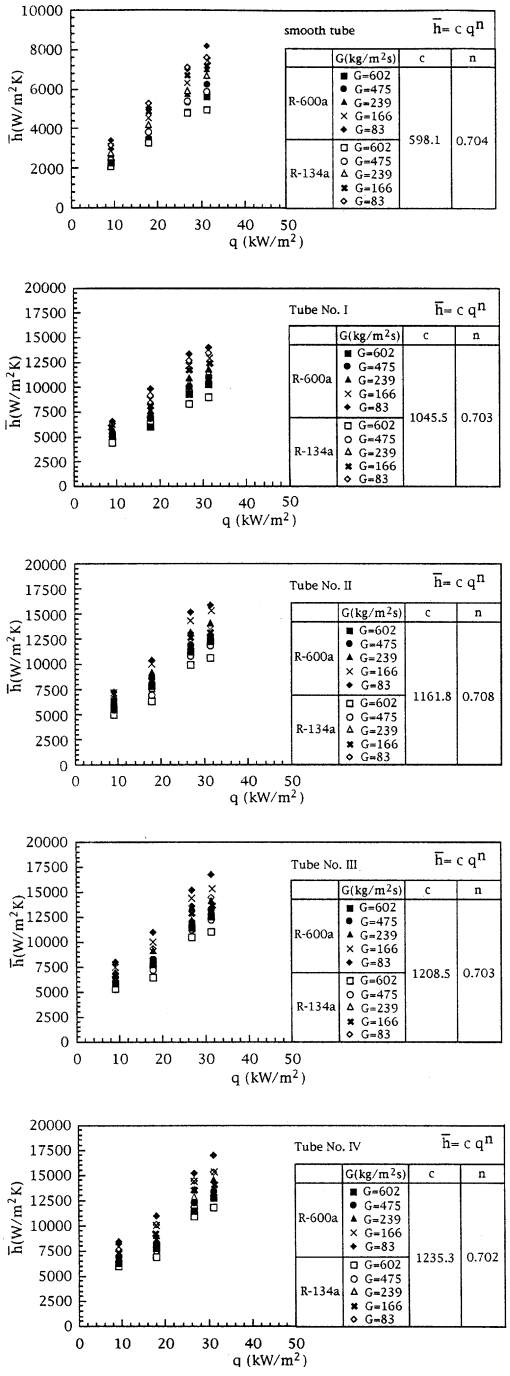

Fig. 7. Average heat transfer coefficient versus heat flux for different tubes.

hole increases. However, the rate of increase seems to decrease and, a plateau eventually seems to be expected.

The insert placement in horizontally and vertically (this study) was examined in a comparison of the present results with those of Hsieh et al. [11] with number of

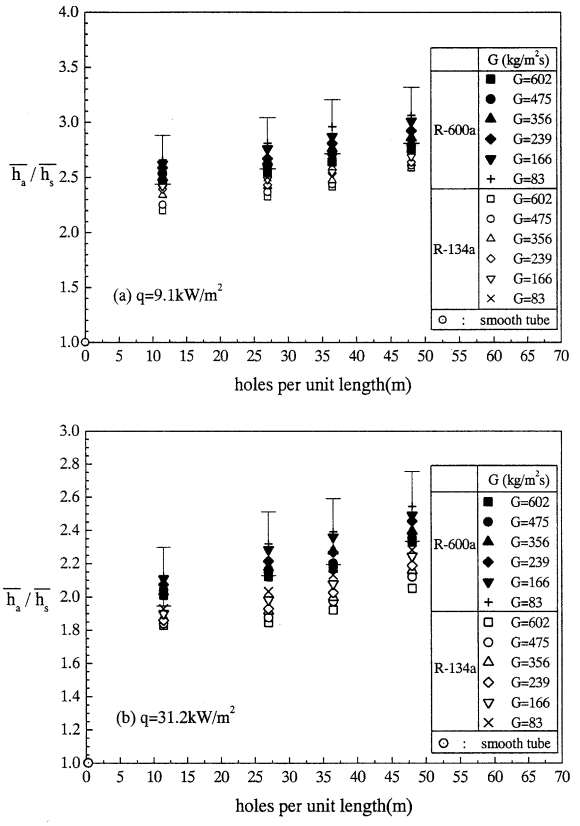

Fig. 8. Average heat transfer enhancement factor vs. unit length of holes for different mass flux at (a) $q = 9.1$ kW/m^2 and (b) $q = 31.2$ kW/m^2.

perforated holes of 23 and 96, and smooth tubes. It was found that the difference cannot be noted. This strongly indicates that the orientation of placement for the inserts seems insignificance. This is perhaps because the present study is dominated either by forced convective evaporation at high quality or by nucleate boiling at low quality. This is different from the traditional single phase flow in which the orientation of test section is quite important. Further and extensive study in this regard is needed.

3.4. Pressure drop results

The two-phase pressure drop was measured across each of the two test sections connected in series. Each test section was 250 mm long for the differential pressure drop measurements. The pressure drop gradients as shown in Fig. 9 are the combined frictional and accelerational components. The inlet and outlet vapor quality is from 0.002 to the exit quality. Generally, pressure drop increases with increasing mass flux, as expected. Based on the rate of increase, it is found from Fig. 9,

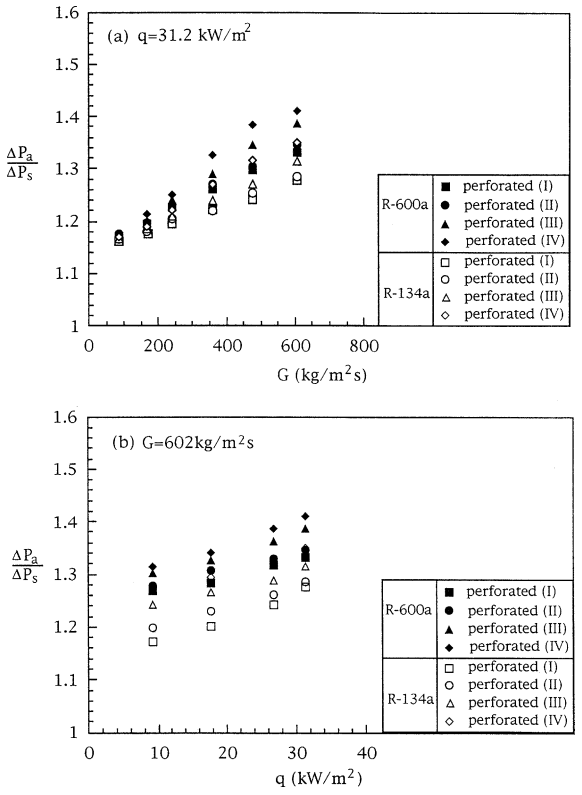

Fig. 9. (a) The pressure gradient ratio vs. mass flux at $q = 31.2$ kW/m^2 and (b) the pressure gradient ratio vs. heat flux at $G = 602$ kg/m^2 s.

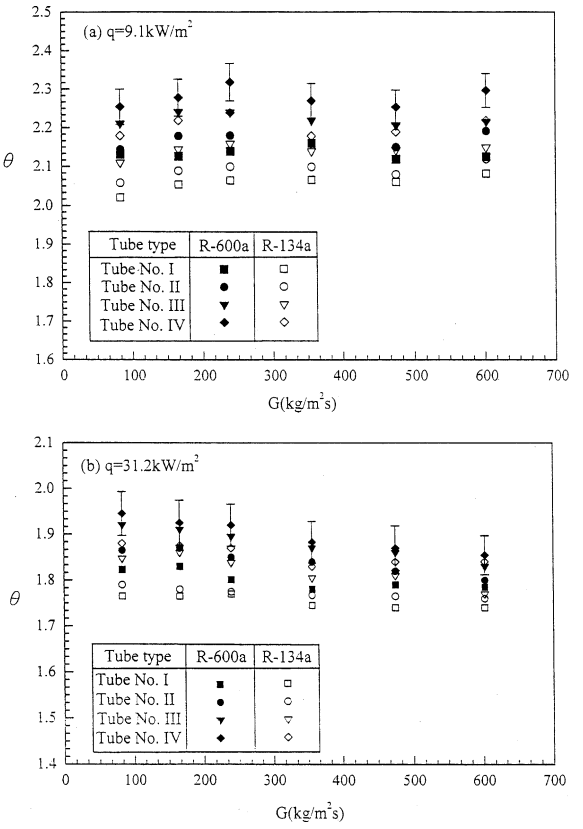

Fig. 10. Enhancement performance ratio for tubes with inserts at (a) $q = 9.1$ kW/m^2 and (b) $q = 31.2$ kW/m^2.

that most of the pressure drop penalty is at high vapor qualities. It is also seen that the pressure drop of the perforated-hole strip is somewhat higher than that of the smooth tube for both R-134a and R-600a due to an increased frictional and form drag. As the number of hole increases, the pressure drop increases. Moreover, the magnitude of the pressure drop is higher for R-600a than for R-134a. The pressure gradient ratios ($\overline{\Delta P}_a/\overline{\Delta P}_s$) found ranged from 1.1 to 1.3 and 1.2–1.4 for R-134a and R-600a, respectively. The pressure gradient ratio is higher as the mass flux increases at a given heat flux. The pressure drop increases over the corresponding smooth tube due to the reduced (by about 5%) cross-sectional flow area. In addition, the difference in magnitude of the pressure gradient ratio is noted at higher heat flux. This is mainly because the acceleration effect was much higher. The same finding is found for different heat fluxes at a given mass flux.

Fig. 10 shows the same evaporation data for the tubes with inserts, but in the form of enhancement performance ratio $\theta(=(\bar{h}_a/\bar{h}_s)/(\overline{\Delta P}_a/\overline{\Delta P}_s))$. It is emphasized that the ratios are based on a comparison of individual data points at different heat flux levels. The maximum was found for tube with 96 perforated hole insert for both R-134a and R-600a, which can be seen from Fig. 10(a) and (b). While heat transfer coefficients increase with increasing mass flux G, there is a tendency for θ to decrease with increasing mass flux G especially at a higher heat flux. At low mass flux, θ has a value (average) of 1.75–1.95 but falls to around 1.7 at a high mass flux as shown in Fig. 10(b). The performance of all four tubes is similar, with a deviation of only 7–12%. Generally speaking, this is approximately the same magnitude as the uncertainty and the θ value seems higher ($\cong$2.2) at low heat flux than that at high heat flux ($\cong$1.8).

3.5. Correlation of heat transfer with relevant parameters (Re_L, Bo, η, and P_R)

There are no available experimental data for published work with inserts like the present one. But, nevertheless, some related works have been studied such as Kandlikar [18], Gungor and Winterton [19], and Liu and Winterton [20]. It is found from Fig. 11 that, these

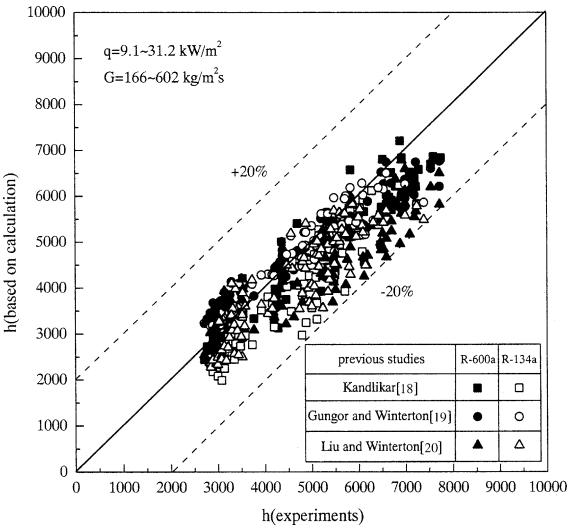

Fig. 11. Comparison of the experimental heat transfer coefficients with those from previous studies.

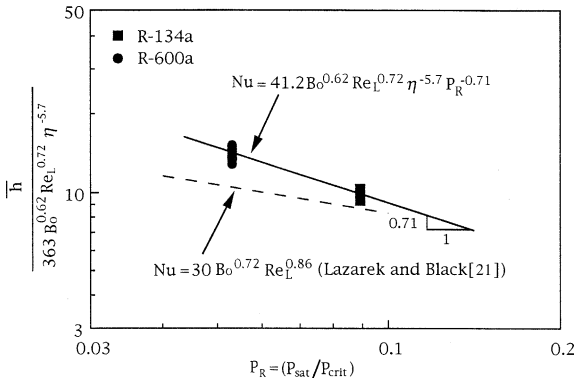

Fig. 12. Correlation of heat transfer coefficients for different refrigerants.

correlations suit well for our R-134a/R-600a flows within ±20%.

As evidenced by the preceding discussion, the heat transfer characteristics are dependent on the quality, which represents different regimes, as well as on the heat flux, mass flux, and the number of perforated holes. Through dimensional analysis, and considering the aforementioned factors, the following dimensionless group, Re, Bo, η, and P_R will be used for correlating the present heat transfer results. The results are also compared with that of Lazarek and Black [21], because of its simple form and easy to implement, as shown in Fig. 12. Again, D_h was used for defining Nu. The equation has the following form:

$$Nu = 41.2Bo^{0.62}Re_L^{0.72}\eta^{-5.7}P_R^{-0.71} \quad (1)$$

where $3.89\times10^{-5} \leqslant Bo \leqslant 1.07\times10^{-3}$; $6000 \leqslant Re_L \leqslant 21,000$; $1.25 \leqslant \eta \leqslant 1.29$; $0.0529 \leqslant P_R \leqslant 0.0892$. Although the range of η tested seems too small to be of significance, the correlation was still made for η for completeness. The power of the term for Re_L and Bo somehow differs from those of Lazarek and Black [21]. The value of coefficient (41.2) of Eq. (1) indicates the enhancement performance and weak dependency of Bo (0.64 for this study) as compared to that corresponding value (=30) of Lazarek and Black's correlation [21]. Furthermore, based on the exponents obtained for each dimensionless parameter, the influence of Re_L, Bo, η and P_R on heat transfer performance is significant. Moreover, the present correlation developed is weakly dependent on mass velocity with a power of 0.10. This is also consistent with the results shown in Fig. 7.

4. Conclusion

Evaporation heat transfer and pressure drop in horizontal tubes with vertically positioned perforated strip-type inserts using R-134a and R-600a have been studied to examine the effect of the relevant parameters of mass flux, heat flux, number of perforated holes of the inserts, and types of refrigerants on the pressure drop and heat transfer coefficient. The important features can be drawn as follows:

(1) The flow pattern map followed by Kattan et al. [15] was developed and was superimposed on the heat transfer data of this study. A demarcation point quality where the onset of the transition form traditional plug/slug or stratified-wavy to the annular flow regime was identified. It is a function of heat flux, mass velocity, number of perforated holes of the inserts, but seems independent of the type of refrigerants.
(2) The effect of mass flux, heat flux, perforated hole, and orientation of the insert placement on heat transfer rates was presented and discussed. It is found that the effect of insert orientation seems insignificance on heat transfer results.
(3) It is found that, both the heat transfer coefficient and pressure drop increased as the number of holes per unit length increases. The enhancement performance ratio has an average value of 1.85 and 2.1 among these four tested tubes at $q = 9.1$ and 31.2 kW/m^2, respectively. It seems there exists a limit enhancement factor at a definite number of holes per unit length as shown in Fig. 8.
(4) The Nusselt number was correlated using a number of relevant parameters as shown in Eq. (1). The effect of perforated holes is obvious, i.e., the exponent of the term of η is −5.7. Moreover, the results were again in good agreement with those of previous

studies as far as the exponents of the term for *Re* and *Bo* was concerned.

References

[1] J.G. Collier, J.R. Thome, Convective Boiling and Condensation, third ed., Oxford University Press, Oxford, 1994.

[2] N. Kattan, J.R. Thome, D. Favrat, Flow boiling in horizontal tubes: Part 2—New heat transfer data for five refrigerants, ASME J. Heat Transfer 120 (1998) 148–155.

[3] N. Kattan, J.R. Thome, D. Favrat, Flow boiling in horizontal tubes: Part 3—Development of a new heat transfer model based on flow pattern, ASME J. Heat Transfer 120 (1998) 156–165.

[4] J.R. Thome, Enhanced Boiling Heat Transfer, Hemisphere Publishing Corporation, Washington DC, 1990.

[5] K. Hambraeus, Heat transfer coefficient during two-phase flow boiling ofs HFC-134a, Int. J. Refrigeration 64 (1991) 357–362.

[6] J.P. Wattelet, J.C. Chato, A.L. Souza, B.R. Christofferson, Evaporation characteristics of R-12, R-134a, and a mixture at low fluxes, ASHRAE Trans. 100 (1992) 603–615.

[7] M. Ito, H. Kimura, Boiling heat transfer and pressure drop in integral spiral-grooved tubes in the region of low how rates, Bull. Jap. Social Mech. Engs. 24 (1979) 1600–1601.

[8] L.M. Schlager, M.B. Pate, A.E. Bergles, Evaporation and condensation heat transfer and pressure drop in horizontal, 12.7 mm micro-fin tubes with refrigerant 22, ASME J. Heat Transfer 112 (1990) 1041–1045.

[9] A. Singh, M.M. Ohadi, E. Dessiatioun, Flow boiling heat transfer coefficients of R-134a in a microfin tube, ASME J. Heat Transfer 118 (1991) 497–499.

[10] X. Liu, Condensing and evaporating heat transfer and pressure drop characteristics of HFC-134a and HCFC-22, ASME J. Heat Transfer 119 (1997) 158–163.

[11] S.S. Hsieh, K.J. Jang, Y.C. Tsai, Evaporation heat transfer and pressure drop in horizontal tubes with strip-type inserts using refrigerant 600a, ASME J. Heat Transfer 122 (2000) 387–391.

[12] S.J. Kline, F.A. McClintock, Describing uncertainties in single-sample experiments, Mech. Eng. 75 (1953) 3–8.

[13] F.W. Dittus, L.M. Boelter, University of California, Berkeley, Publications on Engineering, vol. 2, 1930, p. 443.

[14] V. Gnielinski, New equations for heat and mass transfer in turbulent pipe and channel flow, Int. Chem. Eng. 16 (1976) 359–368.

[15] N. Kattan, J.R. Thome, D. Favrat, Flow boiling in horizontal tubes: Part I—Development of a diabatic two-phase flow pattern map, ASME J. Heat Transfer 120 (1998) 140–147.

[16] S.-S. Hsieh, K.-J. Jang, M.-T. Huang, Evaporative heat transfer and enhancement performance of serpentine tube with strip-type inserts using refrigerant-134a, ASME J. Heat Transfer 121 (1999) 752–757.

[17] Z.Y. Bao, D.F. Fletcher, B.S. Hagnes, Flow boiling heat transfer of freon R 11 and HCFC 123 in narrow passages, Int. J. Heat Mass Transfer 43 (2000) 3347–3358.

[18] S.G. Kandlikar, An improved correlation for predicting two-phase flow boiling heat transfer coefficient in horizontal and vertical tubes, in: Heat Exchangers for Two-Phase Flow Applications, ASME, New York, 1983.

[19] K.E. Gungor, R.H.S. Winterton, A general correlation for flow boiling in tube and annuli, Int. J. Heat Mass Transfer 26 (1986) 351–358.

[20] Z. Liu, R.H.S. Winterton, A general correlation for saturated and subcooled flow boiling in tube and annuli, based on a nucleate pool boiling equation, Int. J. Heat Mass Transfer 34 (1991) 2759–2766.

[21] G.M. Lazarek, S.H. Black, Evaporative heat transfer, pressure drop and critical heat flux in small vertical tube with R-113, Int. J. Heat Mass Transfer 25 (1982) 954–960.

[22] C.Y. Yang, R.L. Webb, Friction pressure drop of R-12 in small hydraulic diameter extruded aluminum tubes with and without micro-fins, Int. J. Heat Mass Transfer 39 (1996) 801–809.